Samd7 is a cell type-specific PRC1 component essential for establishing retinal rod photoreceptor identity

Yoshihiro Omori[a,1], Shun Kubo[a,1], Tetsuo Kon[a], Mayu Furuhashi[a], Hirotaka Narita[b], Taro Kominami[c], Akiko Ueno[a], Ryotaro Tsutsumi[a], Taro Chaya[a], Haruka Yamamoto[a], Isao Suetake[d], Shinji Ueno[c], Haruhiko Koseki[e], Atsushi Nakagawa[b], and Takahisa Furukawa[a,2]

[a]Laboratory for Molecular and Developmental Biology, Institute for Protein Research, Osaka University, Osaka 565-0871, Japan; [b]Laboratory of Supramolecular Crystallography, Institute for Protein Research, Osaka University, Osaka 565-0871, Japan; [c]Department of Ophthalmology, Nagoya University Graduate School of Medicine, Nagoya 466-8550, Japan; [d]Laboratory of Epigenetics, Institute for Protein Research, Osaka University, Osaka 565-0871, Japan; and [e]Laboratory for Developmental Genetics, RIKEN Center for Integrative Medical Sciences, Yokohama 230-0045, Japan

Precise transcriptional regulation controlled by a transcription factor network is known to be crucial for establishing correct neuronal cell identities and functions in the CNS. In the retina, the expression of various cone and rod photoreceptor cell genes is regulated by multiple transcription factors; however, the role of epigenetic regulation in photoreceptor cell gene expression has been poorly understood. Here, we found that Samd7, a rod-enriched sterile alpha domain (SAM) domain protein, is essential for silencing nonrod gene expression through H3K27me3 regulation in rod photoreceptor cells. *Samd7*-null mutant mice showed ectopic expression of nonrod genes including S-opsin in rod photoreceptor cells and rod photoreceptor cell dysfunction. Samd7 physically interacts with Polyhomeotic homologs (Phc proteins), components of the Polycomb repressive complex 1 (PRC1), and colocalizes with Phc2 and Ring1B in Polycomb bodies. ChIP assays showed a significant decrease of H3K27me3 in the genes up-regulated in the *Samd7*-deficient retina, showing that *Samd7* deficiency causes the derepression of nonrod gene expression in rod photoreceptor cells. The current study suggests that Samd7 is a cell type-specific PRC1 component epigenetically defining rod photoreceptor cell identity.

retina | photoreceptor | Polycomb | histone modification | gene silencing

In the vertebrate retina, each rod and cone photoreceptor subtype expresses a distinct set of genes, including the genes encoding phototransduction components such as opsins and transducins. This subtype-specific gene expression is essential for achieving proper functioning in each photoreceptor cell. Numerous studies have demonstrated that the precise expression of photoreceptor subtype-specific genes is achieved by the combinatorial functions of multiple transcription factors (TFs), including photoreceptor TFs such as the pan-photoreceptor TFs Crx, Otx2, and Rorb, the rod-specific TFs Nrl and Nr2e3, and the cone-specific TFs Rora, Thrb2, and Rxrg (1–9). For instance, while the *Rhodopsin* gene is synergistically transactivated by Crx and Nrl in rod photoreceptors, S-opsin (*Opn1sw*) transcription is suppressed by Nr2e3, which interacts with Crx (10, 11). Loss of Nr2e3 or Nrl function in the mouse retina causes ectopic expression of S-opsin in rod photoreceptor cells and dysfunction of rod photoreceptor responses (4, 12, 13). In recent years, genome-wide expression-profile analysis of photoreceptor cells using photoreceptor TF mouse mutants revealed TF networks in the developing retina (14–18). Overall, subtype-specific transcriptional regulation in photoreceptors has been understood mainly from the link between cell type-specific *cis*-regulatory elements and TFs.

Recently, several studies reported dynamic changes in the genome-wide epigenetic landscape of the developing retina (19–23), suggesting that epigenetic control, including histone modification and DNA methylation, has emerged as a potential key mechanism governing gene expression in the developing retina (24). Functions of several histone-modification factors in the retina have been analyzed using animal models. These studies indicate that attenuations of histone modification mainly cause severe defects in early retinal progenitor proliferation and/or in the survival of the mature retina (25–28). Conditional deletion of H3K9 methyltransferase G9a in the developing retina causes significant cell death of differentiated retinal cells due to the aberrant expression of progenitor cell genes, although cell differentiation occurs normally, suggesting that H3K9 methylation marks in progenitor cell genes are essential for the survival of retinal cells (25). Mice with knockout of the H3K4me2/3 demethylase gene *Kdm5b*/*Jarid1b* show anophthalmia or microphthalmia, indicating the essential role of *Kdm5b* in early retinal cell proliferation (26). Polycomb repressive complexes (PRCs) play central roles in the regulation of gene silencing during development through H3K27me3, H2AK119ub, and subsequent chromatin condensation (29, 30). In mouse development, loss of Bmi1, a PRC1 component, causes a slight reduction in retinal cell proliferation (27) and cell death in bipolar and cone photoreceptor cells (28). Conditional deletion of *Ezh2*, encoding a PRC2 component, in the developing mouse retina causes a reduction of retinal progenitor cell proliferation (31).

Significance

Each retinal rod and cone photoreceptor cell subtype expresses a distinct set of genes including the genes encoding phototransduction components such as opsins and transducins. This subtype-specific gene expression is essential for achieving proper function in each photoreceptor cell. While the various cone and rod photoreceptor cell gene expressions are regulated by multiple transcription factors, whether epigenetic regulation plays an important role for photoreceptor cell-specific gene expression has been unclear. In the current study, we found that a photoreceptor-specific protein, Samd7, functions as a component of the epigenetic gene-silencing complex and is essential for establishing rod photoreceptor cell identity and function by silencing nonrod gene expression in developing rod photoreceptor cells.

Knockdown of the H3K27me2/3-specific demethylase Kdm6b/Jmjd3 leads to an impairment of bipolar cell differentiation (32). Despite these studies, the precise contribution of epigenetic regulation in retinal cell differentiation and maturation remains largely unknown.

A homeodomain transcription factor, Otx2, is essential for the cell-fate determination of photoreceptor cells (2, 33). Otx2 conditional knockout (CKO) mice show an almost complete loss of photoreceptors as well as an increase of amacrine cells in the retina. To identify the genes regulating photoreceptor development, we performed microarray analysis using the Otx2 CKO retina and the WT control retina. We observed that two functionally unknown SAM (sterile alpha motif) domain-encoding genes, Samd7 and Samd11/mr-s, were significantly reduced in the Otx2 CKO retina at postnatal day (P) 12 (34, 35). Samd7 (4930597A01Rik) was first reported to be expressed predominantly in the photoreceptor layer of the developing retina (36). Although Samd7 was shown to suppress the Crx-mediated transactivation of Retinoschisin and Samd7 promoters in a reporter assay (37), neither the molecular machinery of transcriptional suppression by Samd7 nor its in vivo function in the retina have yet been reported. Samd7 and Samd11 proteins contain a single SAM domain bearing high similarities to those of Polyhomeotic homologs (Phc). This suggests a possible involvement of these proteins in the machinery of chromatin modifications and transcriptional regulation in postnatal retinal development. In the current study we investigated the biological function and mechanism of Samd7 in the developing retina. We found that Samd7 is a cell type-specific PRC1 component regulating H3K27me3 marks for establishing rod photoreceptor identity and its proper function.

Results

Samd7 Is Expressed in Developing Rod Photoreceptors.
To explore the Samd7 expression pattern in the developing retina, we carried out in situ hybridization using developing and adult mouse retinal sections (Fig. 1A). Samd7 expression was first detected at day P1, a stage at which rod genesis has peaked, in the outer part of the neuroblastic layer containing rod photoreceptor precursor cells (Fig. 1A). Increased Samd7 expression was observed in the outer nuclear layer (ONL) at P6, when rod differentiation is proceeding. Samd7 expression decreased in the ONL after P9 but continued until mice were 4 wk old. Samd7 expression levels were confirmed by Northern blot analysis. Consistent with the results of in situ hybridization and the previous RT-qPCR study (37), we observed that the Samd7 expression level in the retina peaked between P6 and P14 (Fig. S1A). These results indicate that Samd7 is mainly expressed in developing photoreceptors during maturation.

To investigate its localization, we raised an antibody against the Samd7 protein. We immunostained mouse retinal sections at P4 using the anti-Samd7 antibody together with an anti-thyroid hormone receptor β2 (Thrb2) antibody, a marker for cone nuclei. The Samd7 signal specifically localized to the developing ONL (Fig. 1B). While the Samd7 signal was enriched in rods in the ONL, no significant signal was detected in Thrb2-positive cones (Fig. 1B, arrows). We immunostained mouse retinal sections using antibodies against Samd7, Thrb2, and S-opsin. Samd7 becomes
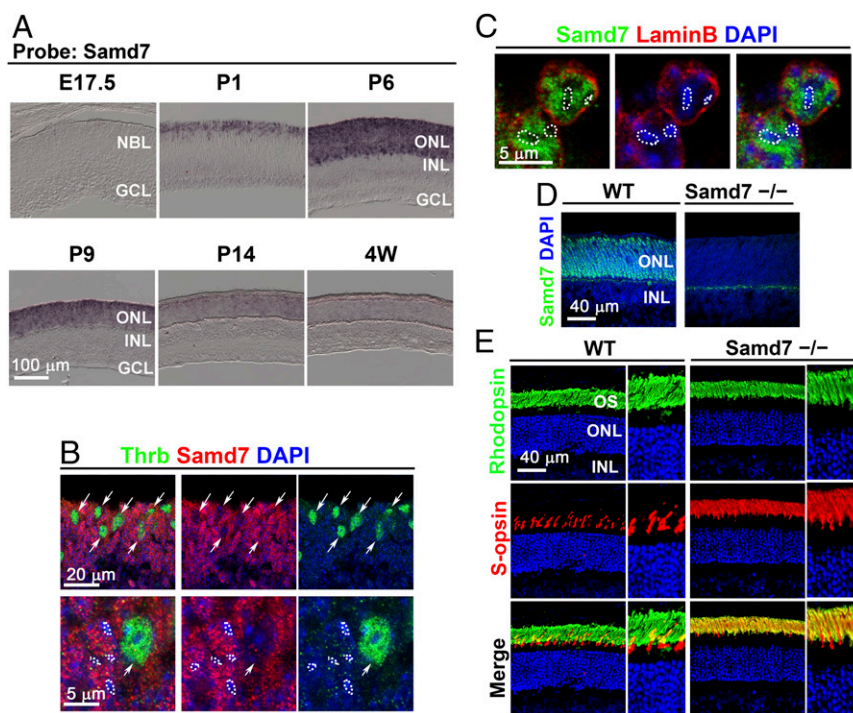
Fig. 1. Samd7 expression and immunostaining of the Samd7−/− retina. (A) In situ hybridization analysis of Samd7 in developing and adult mouse retinas. No Samd7 signal was detected at E17.5, but weak Samd7 expression was observed in the neuroblastic layer at P1. P6 and P9 retinas exhibited Samd7 signals in the prospective photoreceptor layer, and P14 and adult (4 wk, 4W) retinas express Samd7 in the photoreceptor layer. (B) Immunostaining of a P4 WT retinal section using anti-Samd7 (red) and anti-Thrb2 (a cone photoreceptor marker; green) antibodies. Cell nuclei were stained with DAPI. The Samd7 signals did not substantially overlap with Thrb2-positive cone photoreceptor cells (arrows). Dotted lines indicate heterochromatin regions. (C) Samd7 immunostained signals (green) were mainly observed in DAPI (blue)-negative euchromatin regions in the P12 retina. The photoreceptor nuclear membrane was immunostained with the anti-lamin B antibody (red). Dotted lines indicate heterochromatin regions. (D) Retinal sections from WT and Samd7−/− mice at P9 were immunostained using the anti-Samd7 antibody (green) with DAPI (blue). The Samd7 signal in the photoreceptor layer disappeared in the Samd7−/− mice. (E) Retinal sections from adult WT and Samd7−/− mice were immunostained with anti–S-opsin (red) and anti-rhodopsin antibodies (green) with DAPI (blue). Ectopic expression of S-opsin in rod outer segments was observed in the Samd7−/− retina. GCL, ganglion cell layer; INL, inner nuclear layer; NBL, neuroblastic layer; ONL, outer nuclear layer; OS, outer segments.

highly expressed at P6, when S-opsin and Thrb2 can be coimmunostained. We observed faint, background-level Samd7 signals in both S-opsin–positive S-cones and in S-opsin–negative/Thrb2-positive M-cones, which are much weaker than the signals in rods; however, this does not exclude the possibility that Samd7 is expressed at a low level in cones (Fig. S1B). Then we coimmunostained P12 retinal sections with anti-Samd7 and anti-lamin B (a marker for nuclear membrane) antibodies to visualize the rod nucleus along with DAPI, which stains heterochromatin regions. In the rod nuclei, the Samd7 signal barely overlapped with DAPI-positive heterochromatin regions at P4 (Fig. 1B) and P12 (Fig. 1C), suggesting that Samd7 localizes mainly to euchromatin regions in rod nuclei. These results indicate that Samd7 expression is enriched in developing rods and localizes to euchromatin regions.

Samd7 Deletion Causes Ectopic S-Opsin Expression in Rod Photoreceptor Cells. To investigate a possible role for Samd7 in retinal development, we generated Samd7-null mice by targeted gene disruption. We deleted exons 4–6, causing a premature stop codon due to a frame shift, resulting in a SAM domain deletion (Fig. S1C). We confirmed the deletions of Samd7 mRNA and protein in Samd7-null mice by RT-PCR and Western blot, respectively (Fig. S1 D and E). $Samd7^{-/-}$ mice were born in Mendelian ratios, were viable and fertile, and showed no gross morphological abnormalities compared with the WT control mice.

We immunostained retinal sections of WT and $Samd7^{-/-}$ mice at P9 with the anti-Samd7 antibody. Samd7 signals were predominantly observed in the ONL of the WT retina (Fig. 1D). In contrast, no significant Samd7 signal was detected in the $Samd7^{-/-}$ retina. In the mouse retina, rods comprise about 97% of photoreceptor cells (38). Since Samd7 is predominantly expressed in rods, we first investigated the integrity of rod photoreceptors in the $Samd7^{-/-}$ retina. Immunostaining of rod outer segments in the adult mouse retina using an anti-rhodopsin antibody at 10 wk showed no substantial difference between $Samd7^{-/-}$ and WT rod outer segments (Fig. 1E). Next, we immunostained cone outer segments with anti–S-opsin (a blue cone-outer segment marker) and anti–M-opsin (a green cone-outer segment marker) antibodies. In the control retina, both S-opsin and M-opsin signals were observed in a discrete pattern (Fig. 1E and Fig. S2A), reflecting cones' comprising 3% of photoreceptors. Notably, in the $Samd7^{-/-}$ retina strong S-opsin signals were observed in rod outer segments in addition to the cone outer segments (Fig. 1E). In contrast, M-opsin signals were similar in WT and $Samd7^{-/-}$ retinas (Fig. S2A). The distribution of S-opsin signals was unaffected in the $Samd7^{+/-}$ retina (Fig. S2B). We then examined S-opsin localization in the $Samd7^{-/-}$ retina at an earlier stage, P9. The ectopic localization of S-opsin in immature rod outer segments was observed in the $Samd7^{-/-}$ retina (Fig. S2C).

In mice, distribution of S-cone photoreceptors is enriched more in the ventral retina, whereas M-cone photoreceptors are distributed more in the dorsal retina (39). We next examined whether ectopic S-opsin expression levels in rods are different in the dorsal and ventral regions of the $Samd7^{-/-}$ retina. We observed no obvious differences between ectopic S-opsin expression levels in the dorsal and ventral regions of the $Samd7^{-/-}$ retina (Fig. S2D). We also analyzed dorsal and ventral expression patterns of M-opsin in the $Samd7^{-/-}$ retina by flat-mount immunostaining and observed that the enriched distribution of M-opsin–positive cones in the dorsal retina was not affected in the $Samd7^{-/-}$ retina (Fig. S2E).

Retinal photoreceptor cells make synaptic contacts with bipolar and horizontal cell terminals and form ribbon synapses in the outer plexiform layer. To examine the integrity of photoreceptor ribbon synapses in the $Samd7^{-/-}$ retina, we immunostained photoreceptor synaptic ribbons using an anti-Ctbp2 antibody (Fig. S2F). We also investigated synaptic contacts between photo-

receptor cell terminals and ON bipolar synaptic dendrite tips in photoreceptor axonal terminals using an antibody against Pikachurin. In the WT rod ribbon synapse, a single ribbon forms a horseshoe-like structure (green in Fig. S2F) with the photoreceptor–bipolar neural cleft stained with Pikachurin (red in Fig. S2F). In the $Samd7^{-/-}$ retina, we observed no obvious change compared with the WT retina. Immunohistochemical examination using anti-Calbindin (a marker for amacrine and horizontal cells), anti-S100b (a marker for Müller glia), anti-Chx10 (a marker for bipolar cells), and anti-Pax6 (a marker for amacrine and ganglion cells) antibodies showed no substantial difference between WT and $Samd7^{-/-}$ retinas at age 2 mo (Fig. S2G).

Nrl- and Nr2e3-mutant mice exhibit excess S-opsin expression and progressive photoreceptor degeneration (4, 40). To test whether photoreceptor degeneration occurs in the $Samd7^{-/-}$ retina, we measured ONL thickness in the $Samd7^{-/-}$ retina at 12 mo. We detected no significant change in the ONL thickness between WT and $Samd7^{-/-}$ retinas (Fig. S2H), suggesting that Samd7 function is not required for the survival of photoreceptors in mice up to age 12 mo.

Samd7 Loss Impairs Rod Photoreceptor Sensitivity. To evaluate the physiological role of Samd7 in the retina in vivo, we analyzed electroretinograms (ERGs) of adult WT and $Samd7^{-/-}$ mice at age 3 mo (Fig. 2 and Fig. S3). The dark-adapted (scotopic) ERGs elicited by seven different stimulus intensities (-6.2, -5.0, -3.8, -2.6, -1.4, -0.2, and $+1.0$ log cd·s·m^{-2}) of white light were evaluated for WT and $Samd7^{-/-}$ mice (Fig. 2 A, C, and D and Fig. S3 A and B). The amplitude of the a-wave, which originates mainly from the activity of rod photoreceptor cells, at $+1.0$ log cd·s·m^{-2} significantly decreased in the $Samd7^{-/-}$ mice compared with that in WT mice (Fig. 2 A and C and Fig. S3A). In the $Samd7^{-/-}$ mice, the amplitude of the b-wave, which represents electrical potentials from rod bipolar cells activated by rod photoreceptor cells, at -2.6 and -1.4 log cd·s·m^{-2} decreased significantly (Fig. 2 A and D and Fig. S3B). These results suggest that $Samd7^{-/-}$ mice were
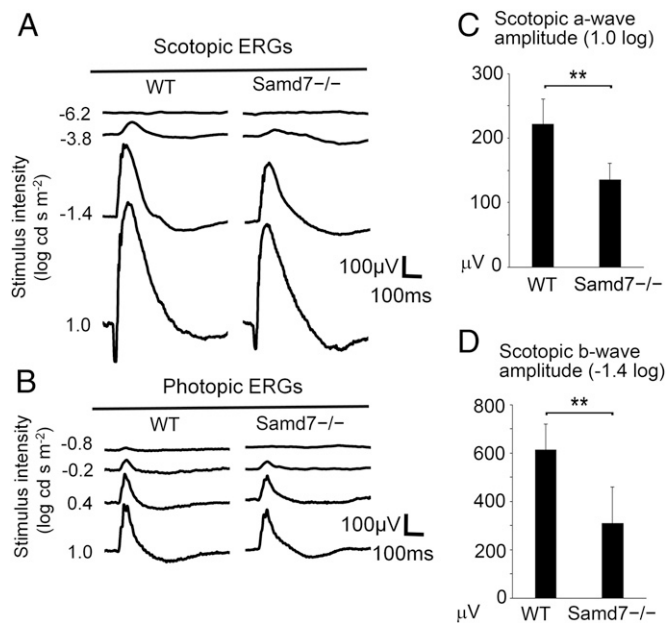
Fig. 2. ERG analysis of $Samd7^{-/-}$ mice. ERGs were recorded from WT (n = 5) and $Samd7^{-/-}$ (n = 5) mice at 12 wk. (A and B) Representative scotopic (A) and photopic (B) ERGs in WT and $Samd7^{-/-}$ mice elicited by white light. (C) The amplitude of the scotopic ERG a-wave as a function of the stimulus intensity (1.0 log cd·s·m^{-2}) was significantly reduced in $Samd7^{-/-}$ mice. (D) The amplitude of the scotopic ERG b-wave as a function of the stimulus intensity (-1.4 log cd·s·m^{-2}) decreased significantly in $Samd7^{-/-}$ mice. Error bars show the SD. **$P < 0.03$.

less sensitive to low-to-moderate flash luminescence than WT mice. On the other hand, the implicit times of the a- and b-waves of the dark-adapted ERGs, which are the speeds of the transduction process in the retina, showed no significant change in the $Samd7^{-/-}$ mice.

Next, we analyzed light-adapted (photopic) ERGs elicited by white light stimuli of four different intensities (−0.8, −0.2, +0.4, and +1.0 log cd·s·m^{-2}). The amplitudes and implicit times of photopic b-waves were not significantly different between WT and $Samd7^{-/-}$ mice (Fig. 2B and Fig. S3C).

Samd7 Deficiency Causes the Dynamic Change of the Transcriptional Profile in the Retina. We observed aberrant expression of *S-opsin* in rod photoreceptors in the $Samd7^{-/-}$ retina. To investigate the genome-wide gene-expression profiles caused by *Samd7* deficiency in the retina, we performed microarray analyses using DNA microarrays containing ≈60,000 probe sets covering 39,430 Entrez Gene RNAs (Agilent Technologies). We compared the expression profiles of WT and $Samd7^{-/-}$ retinas at P12 and identified 163 up-regulated genes (signal log ratio greater than +1.0) and 251 down-regulated genes (signal log ratio less than −0.5) in the $Samd7^{-/-}$ retina (Fig. 3A and Datasets S1 and S2). A previous study reported gene-expression profiles of rod and cone photoreceptor cells by performing RNA-sequencing (RNA-seq) analysis on purified rod and cone photoreceptors (22). Based on fragments per kilobase of exon per million fragments mapped (FPKM) values, we extracted rod- and cone-enriched genes (*Methods*). Among the up-regulated genes in the $Samd7^{-/-}$ retina,
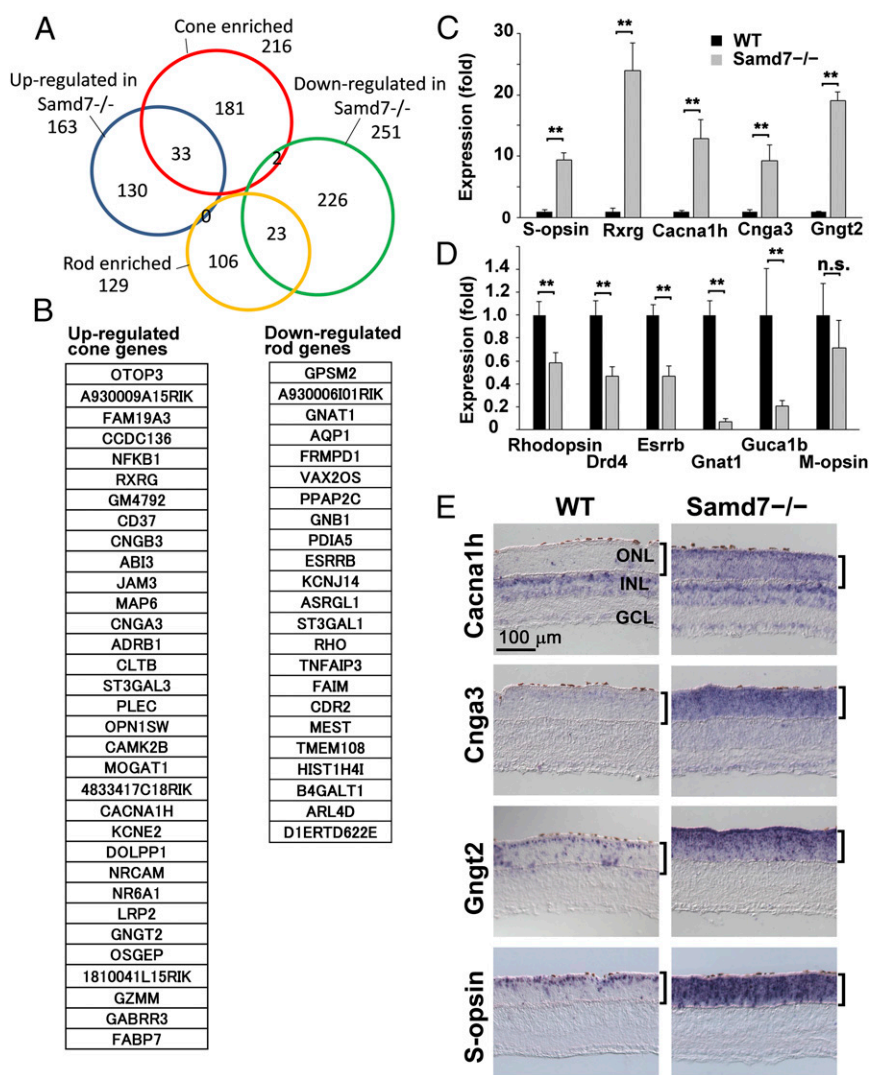
Fig. 3. Global change of retinal expression profile in the $Samd7^{-/-}$ retina. (A) Venn diagram of up-regulated (blue circle) and down-regulated (green circle) genes in the $Samd7^{-/-}$ retina and cone-enriched (red circle) and rod-enriched (yellow circle) genes. Microarray analysis was performed using mRNAs from the WT and $Samd7^{-/-}$ retinas at P12. One hundred sixty-three genes were up-regulated (signal log ratio greater than +1.0, blue circle), and 251 genes were down-regulated (signal log ratio less than −0.5, green circle) in the $Samd7^{-/-}$ retina compared with those in the WT retina. (B) Lists of the 33 genes that overlap between cone-enriched genes and up-regulated genes in the $Samd7^{-/-}$ retina (*Left*) and the 23 genes that overlap between rod-enriched genes and down-regulated genes in the $Samd7^{-/-}$ retina (*Right*). Cone- and rod-enriched genes (more than fourfold FPKM value) were identified using RNA-seq data from a previous study (22). (C and D) The expression levels of the selected genes were measured by qRT-PCR using mRNAs of WT and $Samd7^{-/-}$ retinas at P12. Up-regulation of nonrod genes (C) and down-regulation of rod genes (D) in the $Samd7^{-/-}$ retina by microarray analysis were confirmed. (E) Nonrod genes are ectopically expressed in the ONL of the $Samd7^{-/-}$ retina. In situ hybridization analysis of WT and $Samd7^{-/-}$ retinal sections at P12 was performed using probes for the up-regulated genes in the $Samd7^{-/-}$ retina: *Cacna1h* (a bipolar cell gene), *Gngt2*, *Cnga3*, and *S-opsin* (cone-specific genes). The vertical brackets indicate the extent of the ONL. GCL, ganglion cell layer; INL, inner nuclear layer; ONL, outer nuclear layer. Error bars show the SD ($n = 4$). **$P < 0.03$. n.s., not significant.

33 genes are cone-enriched genes, and among the down-regulated genes in the *Samd7⁻/⁻* retina 23 genes are rod-enriched genes (Fig. 3 *A* and *B*). We also found that the 163 up-regulated genes in the *Samd7⁻/⁻* retina contain various nonrod retinal genes: bipolar cell genes (*Cacna1h*, *gng13*), a ganglion cell gene (*Sema7a*), a ganglion and developing amacrine cell gene (*Robo3*), and a retinal pigment epithelium (RPE)- and cone-enriched gene (*Kcne2*), as well as nonretinal genes, i.e., a stem cell gene (*Pou5f1*), a cardiac- and brain-enriched gene (*Hopx*), and a testicular gene (*Aldoart2*).

To confirm the differential expression of the genes involved in photoreceptor and bipolar functions between WT and *Samd7⁻/⁻* retinas, we selected 11 genes and examined their expression levels by qRT-PCR analysis. Consistent with the results of microarray anal-

ysis, we confirmed that the expression levels of the genes involved in cone (*S-opsin*, *Rxrg*, *Cnga3*, *Gngt2*) and cone bipolar cell (*Cacna1h*) functions were markedly increased in the *Samd7⁻/⁻* retina (Fig. 3*C*). In contrast, expression levels of the genes involved in rod photoreceptor function (*Rho*, *Drd4*, *Esrrb*, *Gnat1*, *Guca1b*) were significantly decreased in the *Samd7⁻/⁻* retina (Fig. 3*D*). *M-opsin* expression exhibited no significant change in the *Samd7⁻/⁻* retina.

We then confirmed the expression pattern of the genes up-regulated in the *Samd7⁻/⁻* retina by in situ hybridization. In the WT retina at P12, the *Cacna1h* signal was observed in the inner nuclear layer (INL) (Fig. 3*E*). In the *Samd7⁻/⁻* retina, we observed that *Cacna1h* was ectopically expressed in the ONL in addition to the INL expression (Fig. 3*E*). While weak signals of the cone-specific

Fig. 4. Samd7 interacts with Phc proteins in PRC1 and a rod TF Nr2e3. (*A*) Yeast two-hybrid assay using full-length *Samd7* as the bait. Proteins containing SAM domains with high similarity to Samd7 (Samd7/11, Phc1/2/3, and L3mbtl3) were identified as Samd7 interactor proteins. Growth on selective plates lacking histidine (–His) and adenine indicates a physical interaction between the bait and prey constructs. (*B*) Immunoprecipitation analysis of Samd7 and Phc2. A plasmid expressing FLAG-Samd7 or FLAG-Phc2 was transfected with a plasmid expressing GFP-Samd7 into HEK293 cells. FLAG-tagged proteins were immunoprecipitated using an anti-FLAG antibody. GFP-Samd7 was coimmunoprecipitated with FLAG-Samd7 or FLAG-Phc2. (*C*) Immunoprecipitation was performed using mouse retinal lysate from 2-mo-old mice using an anti-Phc2 antibody. Immunoprecipitated Samd7 with Phc2 was detected by Western blot analysis using the anti-Samd7 antibody. (*D*) A 3D structural model of the EH and ML surfaces of the Samd7 SAM domain. The putative 3D structure of the Samd7 SAM domain was obtained by MODELLAR (https://salilab.org/modeller/) using the Phc3 SAM domain as a template [Protein Data Bank (PDB) ID code 4PZN]. Two molecules of the Samd7 SAM domain (green and blue) are shown. Amino acids essential for interaction on the EH surface (L372) and the ML surface (L358/H363) are indicated in red. (*E*) Immunoprecipitation of FLAG-Samd7-WT with GFP-Samd7-WT or GFP-Samd7-LR (with the L372R mutation on EH surface of the SAM domain). Reduced interaction between FLAG-Samd7-WT or FLAG-Samd7-LR and GFP-Samd7-LR was observed compared with that between FLAG-Samd7-WT and GFP-Samd7-WT. (*F*) FSEC analysis of the Samd7 protein. Plasmids expressing GFP-fused WT Samd7 (GFP-Samd7-WT) and Samd7 with a mutation on the EH surface of the SAM domain (GFP-Samd7-L372R) were transfected into HEK293 cells, and the fluorescent signals in lysates were analyzed by FSEC. In GFP-Samd7-WT lysates, a putative monomer peak between the 44- and 158-kDa size markers and a broad peak likely corresponding to polymers larger than 669 kDa (arrowhead) were observed. Putative monomer and oligomer peaks but no obvious peaks at a higher molecular size were detected in GFP-Samd7-L372R lysates. (*G*) Yeast two-hybrid assay using Samd7 with mutations in the SAM domain ML (L358R/H363R, HR) and/or EH (L372R, LR) surfaces as baits. The interaction of Samd7 constructs with SAM domain proteins (Samd7/11, Phc1/2/3, L3mbtl3) was analyzed. Samd7 with mutations both on the ML and EH surfaces (L372R/L358R/H363R, LRHR) showed no interaction with any of the SAM domain proteins tested (Samd7/11, Phc1/2/3, L3mbtl3). (*H*) Immunoprecipitation analysis of Samd7 with rod photoreceptor transcription factors. A plasmid expressing FLAG-Samd7 was transfected with a plasmid expressing HA-Nr2e3 or HA-Nrl into HEK293 cells. FLAG-tagged Samd7 was immunoprecipitated using an anti-FLAG antibody. The interaction of Samd7 with Nr2e3 was observed, whereas Samd7 showed no substantial interaction with Nrl.

genes *Cnga3*, *Gngt2*, and *S-opsin* were observed in the outer part of the ONL in the WT retina, the *Samd7*$^{-/-}$ retina exhibited strong *Cnga3*, *Gngt2*, and *S-opsin* expression throughout the entire ONL, consistent with the distribution of rod photoreceptors (Fig. 3*E*). Notably, both *Gngt2* and *S-opsin* showed generally weak expression with strongly expressed points scattered throughout the entire ONL, suggesting that most rods in the *Samd7*$^{-/-}$ retina express these two genes but at variable rather than uniform expression levels. These results indicate that *Samd7* is needed to suppress various nonrod genes expressed both in the retina and outside the retina.

Samd7 Interacts with PRC1 Components, Phc1/2/3 Proteins. To elucidate molecular mechanisms of transcriptional repression by Samd7, we performed a yeast two-hybrid screen to identify the factor(s) that interacts with Samd7. A full-length Samd7-coding sequence, fused in-frame with the yeast GAL4 DNA-binding domain, was used to screen a mouse retinal cDNA library. In this screen, we identified several SAM domain proteins, including Samd7/11, Phc1/2/3, and L3mbtl3, as proteins interacting with Samd7 (Fig. 4*A*). The SAM domain of Phc2 showed a high homology with that of Samd7 (56.5% amino acid residue identity). In addition, Phc2 expression in the retina was the highest among the Phc1/2/3 proteins in our microarray data; therefore, we focused on the interaction between Samd7 and Phc2. To test the possible interaction between Samd7 and Phc2, we carried out an immunoprecipitation assay and confirmed a homophilic interaction with Samd7 as well as a heterophilic interaction between Samd7 and Phc2 (Fig. 4*B*). To confirm the endogenous interaction between Samd7 and Phc2, we performed an immunoprecipitation assay using a mouse retinal extract with an anti-Phc2 antibody (Fig. 4*C*). We observed that Samd7 was immunoprecipitated with the anti-Phc2 antibody, suggesting that Samd7 physically interacts with Phc2 in the mouse retina.

To analyze the subnuclear localization of Samd7 and Phc2 in the retina, we immunostained Samd7 and Phc2 in the WT mouse retina at P6 and P12 and at ages 1 and 2 mo (Fig. S4 *A* and *B*). We observed that Samd7 and Phc2 partially colocalized at the surrounding heterochromatin regions of rod photoreceptor nuclei at all stages examined. To examine whether *Samd7* deletion affects the Phc2 localization in photoreceptor cells, we immunostained the retina using antibodies against Samd7 and Phc2 in the *Samd7*$^{-/-}$ retina (Fig. S4*C*). Phc2 localization was unchanged in photoreceptor nuclei in the *Samd7*$^{-/-}$ retina compared with that in the control retina.

A study on the *Drosophila* Ph (dPh) protein revealed that the SAM domain has two different interacting surfaces, the midloop (ML) and end-helix (EH) surfaces, and the SAM domains can bind each other only through ML–EH heterophilic surface interaction (41). It was reported that introduction of mutation(s) in either the ML or EH surface disrupts polymer formation of the SAM domain. In the Phc2 protein, a vertebrate homolog of dPh, a L307R mutation on the EH surface or L293R/H298R on the ML surface disrupts its homophilic interactions (42). Based on amino acid sequence homology, we identified that the L372R mutation on the EH surface and L358R/H363R mutation on the ML surface of Samd7 (Fig. 4*D*) correspond to the L307R mutation on the EH surface and to the L293R/H298R mutation on the ML surface of Phc2, respectively. We examined whether the L372R mutation of Samd7 (Samd7-LR) affects homophilic interaction of Samd7 by immunoprecipitation assay. We observed that the homophilic interactions of Samd7-LR proteins substantially decreased as well as the interactions between Samd7-LR protein and WT Samd7 protein did (Fig. 4*E*), suggesting that the Samd7 protein interaction through ML–EH surface is essential for the homophilic interaction of the Samd7 protein, similar to that of dPh and Phc2 proteins (41, 42).

Polymer Formation of Samd7 Through the SAM Domain. Since both dPh and mammalian Phc proteins containing SAM domains function through polymerization (29, 41, 42), we assessed the polymerization ability of Samd7 through its SAM domain. To test this possibility, we performed fluorescence-detection size-exclusion chromatography (FSEC) analysis. We expressed GFP-fused WT Samd7 (GFP-Samd7-WT) and Samd7 with a L372R mutation in the EH surface of the SAM domain (GFP-Samd7-LR) in HEK293 cells and analyzed the cell lysates by FSEC (43). In GFP-Samd7-WT lysates, we observed the putative monomer peak (between the 44- and 158-kDa size markers) at 43 min and a broad peak (greater than 669 kDa) centered around 28 min (Fig. 4*F*, arrowheads), indicative of putative polymers, in addition to the putative dimer peak at 40 min (Fig. 4*F*). In contrast, we found putative monomer and dimer peaks but no obvious peak of a higher molecular size in the GFP-Samd7-LR lysates. This result showed that Samd7 can self-associate and polymerize through the SAM domain.

Heterophilic Interaction of Samd7 with Phc Proteins. Previous biochemical and structural studies showed that dPh and another SAM domain protein, Scm, form a copolymer through heterophilic interactions of their SAM domains (44, 45). To investigate the heterophilic interactions of Samd7 with Phc proteins, we performed a yeast two-hybrid assay. If the SAM domain of the Phc protein can bind only to either the ML or the EH surface of the Samd7 protein, a single joint copolymer will be formed. In contrast, if the SAM domain-containing Phc proteins can bind to both the ML and EH surfaces, a random copolymer will be formed. To address the possibility of Samd7 copolymer formation, we generated Samd7 mutations in the SAM domain of the ML (L358R/H363R, HR) and/or EH (L372R, LR) surfaces. By using the yeast two-hybrid system, we assayed interactions between Samd7 and each of the SAM domain-containing proteins, Samd7/11, Phc1/2/3, and L3mbtl3, that we identified in our two-hybrid screen of Samd7. We found that Samd7 with triple mutations both in ML and EH surfaces (L372R/L358R/H363R, LRHR) showed no interaction with any of the SAM domain-containing proteins tested (Samd7/11, Phc1/2/3, and L3mbtl3) (Fig. 4*G*). All other Samd7 mutants interacted with all the SAM domain-containing proteins tested. This result suggests the possibility that Samd7 forms random copolymers with various SAM domain-containing proteins.

Samd7 Protein Interacts with Nr2e3 Photoreceptor TF. *Drosophila* orthologs of *Samd7/11* are *Samuel/Moses*, which interact with nuclear receptor DHR78 (46), an ortholog of vertebrate Nr2c1 and Nr2c2, and act as a transcription repressor (47). Loss of nuclear receptor Nr2e3 in mice causes ectopic S-opsin expression in rods similar to that in *Samd7*-null mice (12, 13), suggesting a possible functional link between Samd7 and Nr2e3. To investigate this possibility, we examined whether Samd7 physically interacts with Nr2e3. We transfected a plasmid expressing FLAG-tagged Samd7 together with the plasmids expressing rod photoreceptor transcription factors Nrl or Nr2e3 into HEK293 cells and immunoprecipitated cell lysates with the anti-FLAG antibody. We found that Samd7 interacts with Nr2e3 but not with Nrl (Fig. 4*H*).

We observed decreased expression of multiple rod genes in the *Samd7*$^{-/-}$ retina, suggesting the possibility that Samd7 functions as a transcriptional coactivator in rod photoreceptor cells. To test this possibility, we carried out a luciferase reporter assay. When we transfected a reporter plasmid containing the *Rhodopsin* promoter with Crx and Nrl expression plasmids, the luciferase activity increased markedly, as previously described (Fig. S5*A*) (10, 11). Cotransfection of the Samd7 expression plasmid did not affect the transactivation activity of the *Rhodopsin* promoter by Crx and Nrl (Fig. S5*A*), showing that Samd7 does not exhibit significant cotransactivation activity, at least for the *Rhodopsin* promoter. This result suggests that the reduction of *Rhodopsin* expression in the *Samd7*$^{-/-}$ retina is due to a secondary effect of *Samd7* deficiency.

Phc2-Dependent Colocalization of Samd7 with Ring1B in Polycomb Bodies. PRC1 components form clusters of foci called "Polycomb bodies" in the nuclei of various cells, including ES cells and fibroblasts (48). If Samd7 functions as a PRC1 component, Samd7 should colocalize with Polycomb bodies in the nucleus. To examine this possibility, we expressed a GFP-Samd7 fusion protein with or without FLAG-tagged Phc2 in HEK293 cells. In the absence of Phc2, GFP-Samd7 formed small foci mainly in the cytosol (Fig. S5B). On the other hand, in the presence of Phc2, GFP-Samd7 formed significant foci in the nuclei and colocalized with Phc2 and Ring1B, core components of PRC1 and markers for the Polycomb body (Fig. S5B, arrowheads), showing that Samd7 colocalizes with Polycomb bodies in a Phc2-dependent manner in HEK293 cells.

To investigate the molecular mechanism of Samd7 localization in Polycomb bodies, we then used U2OS human sarcoma cells in which Polycomb bodies have been well characterized (Fig. S5C) (48). We expressed FLAG-tagged Samd7 in U2OS cells and examined the colocalization of Samd7 with Ring1B. In contrast to HEK293 cells, we found that Samd7 colocalized with Ring1B in the nuclear foci without Phc2 overexpression (Fig. S5C). We speculate that Samd7 localizes to Polycomb bodies by using endogenous Phc proteins in the U2OS cells. We found two highly conserved homology domains (HD1 and HD2) in the Samd7 protein, based on amino acid residue homology among species from mouse to zebrafish (Fig. S5D). We prepared Samd7-del1, -del2, and -del3 constructs which lack the HD1, HD2, and SAM domain, respectively. To determine which region of the Samd7 protein is responsible for its localization to Polycomb bodies, we tested the subcellular localization of Samd7-mutant proteins. Similar to WT Samd7, the Samd7-del2 localized to Polycomb bodies (Fig. S5C). The Samd7-del1, -del3, and -LR did not localize to Polycomb bodies and spread throughout the cytosol and nucleus. These results suggest that HD1 and SAM domain are responsible for the Samd7 localization in Polycomb bodies. Interestingly, we also found that higher-level expression of WT Samd7 or the -del1– or -del2–mutant proteins leads to a loss or a depletion of the Ring1B signal in Polycomb bodies (Fig. S5C). In contrast, a higher-level expression of Samd7 without the functional SAM domain (-del3 or -LR) did not cause a depletion of the Ring1B signal (Fig. S5C). This result indicates that Samd7 mutants containing the functional SAM domain showed a dominant negative effect on Polycomb body formation, suggesting that Samd7 can affect polycomb body formation. To examine the indirect physical interaction between Samd7 and Ring1B through Phc2, we performed an immunoprecipitation assay in HEK293 cells. We observed that FLAG-Samd7 interacts with Myc-Ring1B in a Phc2-dependent manner (Fig. S5E).

We next investigated whether Samd7 colocalizes with Polycomb-related marker proteins including Suz12 (a PRC2 component), H3K27me3, and H2AK119ub in U2OS cells (Fig. S5F). As expected, Samd7 partially colocalized with puncta of Suz12, H3K27me3, and H2AK119ub signals in cell nuclei. In contrast, the active H3K4me3 histone mark did not colocalize with Samd7-positive puncta in cell nuclei. These results also support the hypothesis that Samd7 is a functional component of PRC1 in Polycomb bodies.

Samd7 with PRC1 Promotes H3K27me3 Marks in Nonrod Genes. Since Samd7 forms a complex with PRC1 by interacting with Phc proteins, we hypothesized that Samd7 regulates gene expression through histone modification controlled by PRCs. PRC1 deficiency decreases H3K27me3 and/or H2AK119ub marks, because PRC1 and PRC2 cooperatively perform histone modifications on their target genes (29). Samd7 begins to be expressed in rod photoreceptors around P1 (Fig. 1A). If Samd7 represses gene transcription through histone modification of H3K27me3 by the PRCs' machinery in rod photoreceptors, H3K27me3 marks of Samd7 target gene loci would be expected to increase at postnatal stages. To test this hypothesis, we analyzed a level of the H3K27me3 marks for up-regulated genes in the $Samd7^{-/-}$ retina using the previously reported ChIP-sequencing

(ChIP-seq) data in rod photoreceptors at P2, P10, and P28 (21). In rod photoreceptors at P10, 2,235 genes were marked with H3K27me3. We compared these genes with the genes up-regulated in $Samd7^{-/-}$ retina in silico. We found that 36% of the up-regulated genes (58 genes) in the $Samd7^{-/-}$ retina had H3K27me3 marks in rod photoreceptors at P10.

The genomic loci of S-opsin (21), Cnga3 (Fig. 5A), and Cacna1h (Fig. 5B) exhibited low levels of H3K27me3 at P2; however, at P10 they become marked with H3K27me3. Similar to these genes, 181 genes had a more than twofold increase in H3K27me3 at P10 compared with P2 (Fig. 5C). We found that 21% of the genes with elevated H3K27me3 (31 genes) were up-regulated in the $Samd7^{-/-}$ retina. These results suggest that Samd7 and other epigenetic molecules are involved in the developmental up-regulation of H3K27me3.

To confirm whether Samd7 deletion affects H3K27me3 marks on the genes up-regulated in the $Samd7^{-/-}$ retina, we carried out ChIP analysis on selected gene loci. We found that the genes up-regulated in the $Samd7^{-/-}$ retina, including Cacna1h, Cnga3, Gngt2, En2, S-opsin, and Rxrg, exhibited a significant reduction of the H3K27me3 marks in the $Samd7^{-/-}$ retina at P12 (Fig. 5D). In contrast, no obvious H3K27me3 change was detected for Gnat2 and Hoxc13, whose expression levels were unchanged or down-regulated in the $Samd7^{-/-}$ retina, respectively. These results agree with our hypothesis that Samd7 silences nonrod genes by elevating H3K27me3 marks at their target genes in rod photoreceptors.

To investigate whether Samd7 deletion affects H2AK119ub marks on the genes up-regulated in the $Samd7^{-/-}$ retina, we carried out a ChIP-qPCR analysis using an anti-H2AK119ub antibody. We found that the genes up-regulated in the $Samd7^{-/-}$ retina, including Cacna1h, S-opsin, Cnga3, and En2, exhibited a significant reduction of the H2AK119ub marks in the $Samd7^{-/-}$ retina at P12 (Fig. 5 E and F), suggesting that Samd7 also regulates H2AK119ub on the genes up-regulated in the $Samd7^{-/-}$ retina.

Discussion

The Functional Mechanism of the Samd7–PRC1 Complex in Rod Development. Based on our results in this study and previous reports, our proposed model is that Samd7 silences the transcription of nonrod genes as a component of the PRC1 through interaction with photoreceptor transcription factors in rod photoreceptor cells (Fig. S6). In vertebrates, PRC1 is categorized into the canonical PRC1 containing Cbx and Phc proteins and the variant PRC1 containing either RYBP or YAF2 (30, 49). The variant PRC1 is proficient at catalyzing H2AK119ub on chromatin, whereas the canonical PRC1 has limited capacity to deposit H2AK119ub (50). The canonical PRC1 leads to chromatin compaction and gene silencing through Phc–SAM domain clustering (42). This is consistent with PRC1's role in chromatin compaction independent of histone ubiquitination (51). We identified a physical interaction between Samd7 and Phc proteins, indicating that Samd7 is a cell type-specific component of the canonical PRC1. A major role of the Samd7 component of canonical PRC1 seems to be chromatin compaction through copolymerization with Phc–SAM domain.

In the present study, we found a Samd7 polymerization ability leading to self-association through the SAM domain as well as to direct interaction between Samd7 and other Phc proteins. Previously dPh and mammalian Phc proteins were shown to undergo self-polymerization (41, 42). In addition, copolymerization of dPh with Scm has been reported (44, 45). In accordance with these findings, our results suggest that Samd7 and Phc form copolymer by heterointeraction. What is the biological significance of copolymerization by Samd7 and Phc? One possible role of Samd7-Phc copolymerization is modification of the PRC1 function in transcriptional repression. Interaction of Drosophila Scm with dPh through SAM domains is required for recruiting PcG repression (52). Scm tethered to DNA-binding sites provides a
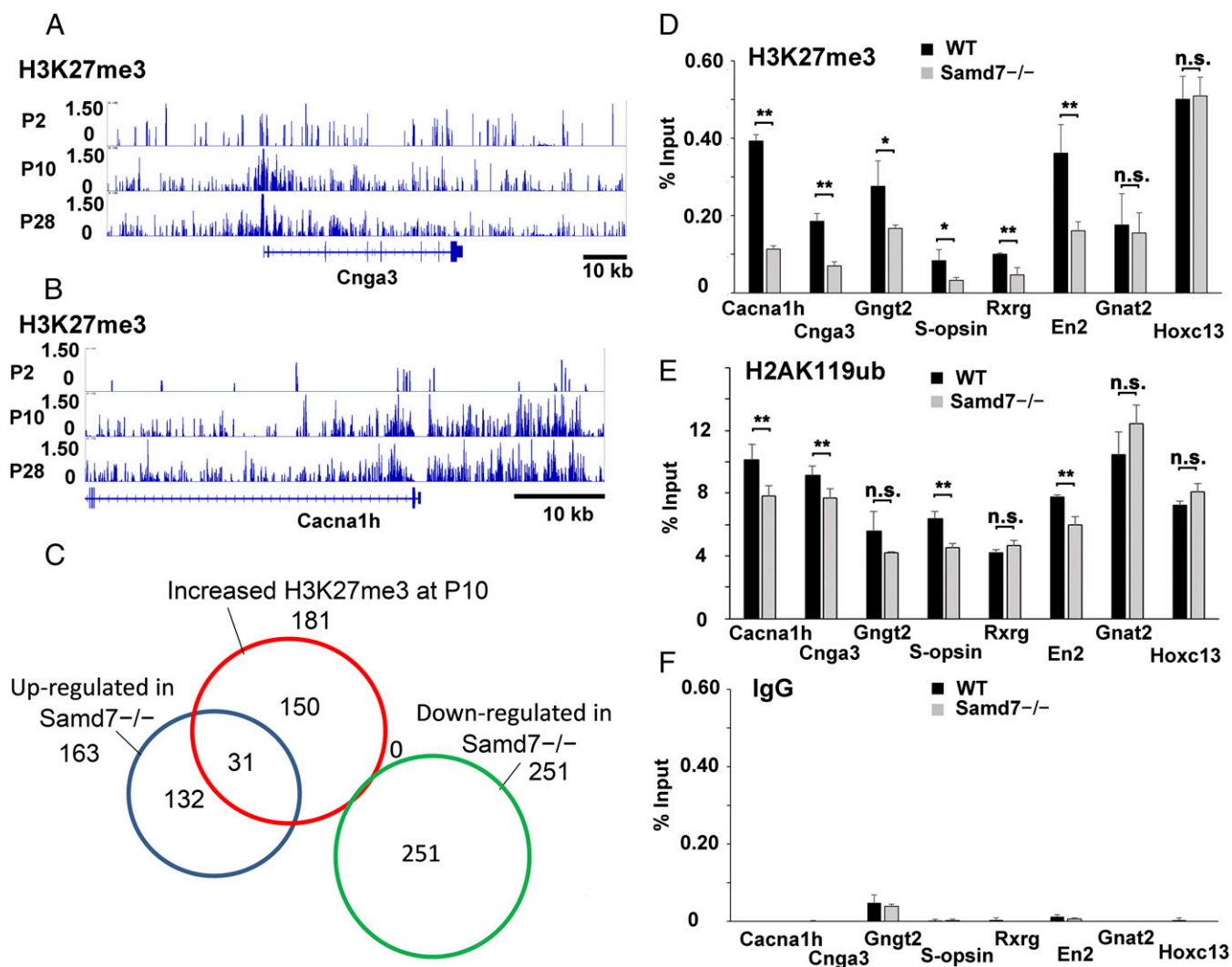
Fig. 5. Samd7 regulates H3K27me3 in the retina. (*A* and *B*) ChIP-seq profiles of *Cnga3* (*A*) and *Cacna1h* (*B*) loci for H3K27me3 in developing rod photo-receptor cells at three different stages (P2, P10, and P28). H3K27me3 levels at *Cnga3* and *Cacna1h* genes, which were up-regulated in the *Samd7$^{-/-}$* retina, increased along with rod photoreceptor development. The ChIP-seq profiles were analyzed using previous ChIP-seq data (21). (*C*) A Venn diagram of up-regulated (blue circle) and down-regulated (green circle) genes in the *Samd7$^{-/-}$* retina and the genes with increased H3K27me3 marks in the developing rods (red circle). Thirty-one genes overlapped between the up-regulated genes in the *Samd7$^{-/-}$* retina and the genes with increased H3K27me3 marks in de-veloping rods. (*D–F*) ChIP-qPCR analysis of H3K27me3 (*D*) and H2AK119ub (*E*) on the selected up-regulated genes in *Samd7$^{-/-}$* retinas. H3K27me3 levels of the selected genes in WT and *Samd7$^{-/-}$* retinas were analyzed by ChIP-qPCR. The H3K27me3 levels of the selected up-regulated genes (*Cacna1h*, *Cnga3*, *Gngt2*, *En2*, *S-opsin*, and *Rxrg*) in WT and *Samd7$^{-/-}$* retinas are indicated. No significant change in H3K27me3 levels was observed for the *Hoxc13* and *Gnat2* pro-moters. The H2AK119ub levels of the selected up-regulated genes in the *Samd7$^{-/-}$* retina (*Cacna1h*, *Cnga3*, *En2*, and *S-opsin*) significantly decreased in the *Samd7$^{-/-}$* retina. (*F*) ChIP with IgG was performed as a negative control. Error bars show the SD ($n = 3$). **$P < 0.03$, *$P < 0.05$. n.s., not significant.

mechanism for long-range transcriptional repression on chro-mosomes (53). Hence, transcriptional repression by Scm is de-pendent on the SAM domain and Ph function. Similar to this model, we propose that Samd7–Phc copolymerization changes physical features of PRC1 such as the distance and/or level of transcriptional repression on chromosomes by chromatin modi-fication. Current results suggest that copolymer formation by Samd7 and other SAM domain proteins plays an essential role in the suppression of nonrod genes in rod photoreceptor cells.

We observed that *Samd7* expression levels decrease remark-ably after the maturation of rod photoreceptor cells (Fig. 1*A* and Fig. S1*A*). This result together with other observations in the current study raises the possibility that *Samd7* is not required for the maintenance of H3K27me3 marks in the adult retina. This could be clarified in a future study by analyzing the effect of induced deletion of *Samd7* on H3K27me3 marks after the matu-

ration of photoreceptor cells using the previously reported the Crx-CreERT2 mouse system (54), in which Cre recombinase activity can be induced upon tamoxifen administration in photoreceptor cells.

We observed rod-enriched Samd7 expression at P4, P6, and 1 mo (Fig. 1*B* and Figs. S1*B* and S4*B*). While Samd7 expression is obviously weaker in cones than in rods at these stages, there is a possibility that *Samd7* is expressed at a low level in cones. Several previous studies reported evidence suggesting Samd7 ex-pression in cones. Mo et al. (22) carried out an RNA-seq analysis of rods and cones collected by FACS. In this analysis, *Samd7* was enriched in rods, but *Samd7* expression was also detected in cones at a lower level than in rods ($\approx$45% of the rod expression level). In the *Nrl$^{-/-}$* retina, the expression of many rod-specific genes almost disappeared; however, *Samd7* expression remained $\approx$60% of that in the WT retina at P21, supporting the possibility of *Samd7* ex-pression in cones (14). Therefore, *Samd7* is likely to be weakly

expressed in cones, implying that Samd7 has a function in cones. However, because the number of cones is only 3% of rods, gene-expression changes in cones in the $Samd7^{-/-}$ retina are unlikely to be detectable by gene-expression analysis using whole retinas. Analysis of expression profiling of cones purified by FACS from the $Samd7^{-/-}$ retina may answer this question in a future study.

Target Specificity of Transcriptional Repression by PRC1 and Samd7. Our microarray analysis showed that Samd7 regulates only a subset of the total PRC1 target genes in rod photoreceptor cells. How is the target specificity of transcriptional repression by Samd7 established? In *Drosophila*, recruitment of PRC1 to target DNA elements by transcription factors was reported (55). Targeting of PRC1 to Polycomb-responsible element (PRE) is carried out through interaction with Scm, dPh, and another SAM domain protein, Sfmbt (56), which is a subunit of the PRE-binding Pho-repressive complex (PhoRC). PhoRC targets PRC1 to PREs on chromatins through heterointeraction of their SAM domains. In mammals, several transcription factors, including Rest (57), Runx (58), and E2F6 (59), were reported to regulate the recruitment of PRC1 to chromatins. Multiple pathways and mechanisms appear to contribute to recruiting PRC proteins to their target genes in mammals.

In vertebrates, most of the PRC components have been identified based on homology to their *Drosophila* orthologs (60). *Drosophila* orthologs of *Samd7/11* are *Samuel/Moses*. *Samuel* mutants are partially lethal at around the late third-instar larval stage or early pupal stage and exhibit overgrowth and hyperplasia, although 15% of animals escape to adulthood with no apparent defects (46). Samuel interacts with nuclear receptor DHR78 (46), an ortholog of vertebrate Nr2c1 and Nr2c2, and acts as a transcription repressor (47). Since Samuel has not been reported as a Polycomb component, it will be interesting to find out whether Samuel has a link to the PRC1 function as Samd7 does.

We found that Samd7 interacts with Nr2e3. Our results suggest that Nr2e3 recruits Samd7 with PRC1 to Samd7 target-gene loci, including *S-opsin*. However, we do not exclude the possibility that Samd7 and PRC1 are recruited to their target loci by other TFs. Since the up-regulated genes in the $Samd7^{-/-}$ retina are not simply cone genes, combinations of other multiple TFs interacting with Samd7 might determine the target genes in rod photoreceptors. A recent study reported that repression of *S-opsin* in developing rod photoreceptor cells correlates with an H3K27me3 increase at the *S-opsin* locus (21). However, a precise molecular mechanism underlying this repression remains unknown. Our current study may at least partially explain this mechanism.

Impact of Samd7 Absence on Retinal Function. Our ERG analysis revealed reduced sensitivity of rods to light in the $Samd7^{-/-}$ retina. This phenotypic aspect of $Samd7^{-/-}$ mice may reflect the down-regulation of the genes involved in rod phototransduction (e.g., *Rhodopsin*, *Gnat1*, and *Guca1b*) in $Samd7^{-/-}$ rod photoreceptors. These results raise the possibility that Samd7 functions as a transcriptional coactivator for certain target genes. Nr2e3 is known to function both as a transcriptional repressor and as a transcriptional activator in rod photoreceptor cells (10, 11). Although we observed no significant effect of Samd7 for trans-activation activity of the *Rhodopsin* promoter by Crx and Nrl in a reporter assay, we do not exclude the possibility that Samd7 is involved in transcriptional activation for certain rod genes. It was reported that heteroinsufficiency of *Rhodopsin* causes slow photoreceptor degeneration in mice (61). Although we did not observe significant photoreceptor degeneration in the $Samd7^{-/-}$ retina at 12 mo, the reduction of various rod photoreceptor genes, including *Rhodopsin*, caused by *Samd7* deletion might lead to slow photoreceptor degeneration under different conditions (e.g., in a different genetic background and/or in more aged mice).

$Nrl^{-/-}$ mice exhibit an increased S-cone–mediated ERG response similar to the clinical phenotype of enhanced S-cone

syndrome (ESCS), in which patients have increased sensitivity to blue light (4). In contrast, $Samd7^{-/-}$ mice show a normal S-cone–mediated ERG response in photopic conditions in addition to the increased expression of S-cone phototransduction genes (e.g., *Opn1sw*, *Cnga3*, *Cngb3*, and *Gngt2*). This phenotype may reflect that not all components necessary for the S-cone phototransduction cascade are up-regulated in the $Samd7^{-/-}$ retina. In fact, expression levels of *Gnat2*, *Pde6c*, and *Pde6h* were not significantly changed between WT and $Samd7^{-/-}$ retinas in our microarray analysis. Similar to $Samd7^{-/-}$ mice, *Nr2e3*-mutant mice (*rd7*) showed normal S-cone–mediated ERG responses in photopic conditions (62); however, patients with a mutation in *NR2E3* exhibit enhanced S-cone–mediated ERG responses (5), suggesting that some aspects of the phenotype caused by *Nr2e3* loss may be different in humans and mice. Furthermore, mutations in *NR2E3* are associated with ESCS, which manifests as increased sensitivity to blue light and night blindness due to rod loss. In addition, several *NR2E3* mutations were reported to be associated with retinitis pigmentosa (RP) (63). Likewise, we propose that *SAMD7* absence in humans may cause retinal diseases, including ESCS and RP. Since mutations in noncoding *cis*-regulatory variants in CRX-binding regions of human *SAMD7* have been found in autosomal recessive RP patients (64), the current study suggests a possible involvement of *SAMD7* in ESCS and/or RP pathogenesis.

We previously reported that *Samd11*, a putative *Samd7* paralog, is highly enriched in photoreceptors (34). While transcriptional repressive activities of Samd7 and Samd11 were observed by luciferase reporter assay in cultured cells (34, 37), the present study suggests that Samd7 silences nonrod gene expression as a cell type-specific component of PRC1 in developing rod photoreceptor cells. Since in the current study we found that Samd11 interacts with Samd7 through the SAM domain, it will be particularly interesting to investigate whether Samd11 possesses a similar epigenetic function or has a unique role in photoreceptor cells. Future studies of *Samd11*-null and *Samd7/11* double-null mutant mice may clarify these questions.

Materials and Methods

Generation of $Samd7^{-/-}$ Mice. We obtained *Samd7* genomic clones from a screen of the *129S6/SvEvTac* mouse genomic DNA library. We obtained ~5.1-kb and ~5.3-kb *Samd7* genomic fragments from the *Samd7* genomic clone and subcloned the fragments into a modified pPNT vector (Fig. S1C). We transfected the linearized targeting construct into a *129S6/SvEvTac*-derived TC1 ES cell line. The culture, electroporation, and selection of ES cells were performed as described previously (65). ES cells that were heterozygous for the targeted gene disruption were microinjected into blastocysts from ICR females to obtain chimeric mice.

Animal Care. All procedures conformed to the Statement for the Use of Animals in Ophthalmic and Vision Research of the Association for Research in Vision and Ophthalmology, and these procedures were approved by the Institutional Safety Committee on Recombinant DNA Experiments (approval ID 04220) and the Animal Experimental Committee of the Institute for Protein Research (approval ID 29-01-0), Osaka University, and were performed in compliance with the institutional guidelines.

Reagents and procedures including statements of data availability and accession codes are described in detail in *SI Materials and Methods*. Primers used in experiments are described in Table S1.

1. Furukawa T, Morrow EM, Cepko CL (1997) Crx, a novel otx-like homeobox gene, shows photoreceptor-specific expression and regulates photoreceptor differentiation. *Cell* 91:531–541.
2. Nishida A, et al. (2003) Otx2 homeobox gene controls retinal photoreceptor cell fate and pineal gland development. *Nat Neurosci* 6:1255–1263.
3. Furukawa T, Morrow EM, Li T, Davis FC, Cepko CL (1999) Retinopathy and attenuated circadian entrainment in Crx-deficient mice. *Nat Genet* 23:466–470.
4. Mears AJ, et al. (2001) Nrl is required for rod photoreceptor development. *Nat Genet* 29:447–452.
5. Haider NB, et al. (2000) Mutation of a nuclear receptor gene, NR2E3, causes enhanced S cone syndrome, a disorder of retinal cell fate. *Nat Genet* 24:127–131.
6. Roberts MR, Hendrickson A, McGuire CR, Reh TA (2005) Retinoid X receptor (gamma) is necessary to establish the S-opsin gradient in cone photoreceptors of the developing mouse retina. *Invest Ophthalmol Vis Sci* 46:2897–2904.
7. Jia L, et al. (2009) Retinoid-related orphan nuclear receptor RORbeta is an early-acting factor in rod photoreceptor development. *Proc Natl Acad Sci USA* 106:17534–17539.
8. Fujieda H, Bremner R, Mears AJ, Sasaki H (2009) Retinoic acid receptor-related orphan receptor alpha regulates a subset of cone genes during mouse retinal development. *J Neurochem* 108:91–101.
9. Roberts MR, Srinivas M, Forrest D, Morreale de Escobar G, Reh TA (2006) Making the gradient: Thyroid hormone regulates cone opsin expression in the developing mouse retina. *Proc Natl Acad Sci USA* 103:6218–6223.
10. Peng GH, Ahmad O, Ahmad F, Liu J, Chen S (2005) The photoreceptor-specific nuclear receptor Nr2e3 interacts with Crx and exerts opposing effects on the transcription of rod versus cone genes. *Hum Mol Genet* 14:747–764.
11. Cheng H, et al. (2004) Photoreceptor-specific nuclear receptor NR2E3 functions as a transcriptional activator in rod photoreceptors. *Hum Mol Genet* 13:1563–1575.
12. Corbo JC, Cepko CL (2005) A hybrid photoreceptor expressing both rod and cone genes in a mouse model of enhanced S-cone syndrome. *PLoS Genet* 1:e11.
13. Chen J, Rattner A, Nathans J (2005) The rod photoreceptor-specific nuclear receptor Nr2e3 represses transcription of multiple cone-specific genes. *J Neurosci* 25:118–129.
14. Hsiau TH, et al. (2007) The cis-regulatory logic of the mammalian photoreceptor transcriptional network. *PLoS One* 2:e643.
15. Blackshaw S, Fraioli RE, Furukawa T, Cepko CL (2001) Comprehensive analysis of photoreceptor gene expression and the identification of candidate retinal disease genes. *Cell* 107:579–589.
16. Carter TA, et al. (2005) Mechanisms of aging in senescence-accelerated mice. *Genome Biol* 6:R48.
17. Corbo JC, et al. (2010) CRX ChIP-seq reveals the cis-regulatory architecture of mouse photoreceptors. *Genome Res* 20:1512–1525.
18. Hao H, et al. (2012) Transcriptional regulation of rod photoreceptor homeostasis revealed by in vivo NRL targetome analysis. *PLoS Genet* 8:e1002649.
19. Aldiri I, et al. (2015) Brg1 coordinates multiple processes during retinogenesis and is a tumor suppressor in retinoblastoma. *Development* 142:4092–4106.
20. Popova EY, et al. (2012) Stage and gene specific signatures defined by histones H3K4me2 and H3K27me3 accompany mammalian retina maturation in vivo. *PLoS One* 7:e46867.
21. Kim JW, et al. (2016) Recruitment of rod photoreceptors from short-wavelength-sensitive cones during the evolution of nocturnal vision in mammals. *Dev Cell* 37:520–532.
22. Mo A, et al. (2016) Epigenomic landscapes of retinal rods and cones. *Elife* 5:e11613.
23. Ueno K, et al. (2016) Transition of differential histone H3 methylation in photoreceptors and other retinal cells during retinal differentiation. *Sci Rep* 6:29264.
24. Rao RC, Hennig AK, Malik MT, Chen DF, Chen S (2011) Epigenetic regulation of retinal development and disease. *J Ocul Biol Dis Infor* 4:121–136.
25. Katoh K, Yamazaki R, Onishi A, Sanuki R, Furukawa T (2012) G9a histone methyltransferase activity in retinal progenitors is essential for proper differentiation and survival of mouse retinal cells. *J Neurosci* 32:17658–17670.
26. Albert M, et al. (2013) The histone demethylase Jarid1b ensures faithful mouse development by protecting developmental genes from aberrant H3K4me3. *PLoS Genet* 9:e1003461.
27. Chatoo W, Abdouh M, Duparc RH, Bernier G (2010) Bmi1 distinguishes immature retinal progenitor/stem cells from the main progenitor cell population and is required for normal retinal development. *Stem Cells* 28:1412–1423.
28. Barabino A, et al. (2016) Loss of Bmi1 causes anomalies in retinal development and degeneration of cone photoreceptors. *Development* 143:1571–1584.
29. Entrevan M, Schuettengruber B, Cavalli G (2016) Regulation of genome architecture and function by Polycomb proteins. *Trends Cell Biol* 26:511–525.
30. Blackledge NP, Rose NR, Klose RJ (2015) Targeting Polycomb systems to regulate gene expression: Modifications to a complex story. *Nat Rev Mol Cell Biol* 16:643–649.
31. Iida A, et al. (2015) Roles of histone H3K27 trimethylase Ezh2 in retinal proliferation and differentiation. *Dev Neurobiol* 75:947–960.
32. Iida A, et al. (2014) Histone demethylase Jmjd3 is required for the development of subsets of retinal bipolar cells. *Proc Natl Acad Sci USA* 111:3751–3756.
33. Sato S, et al. (2007) Dkk3-Cre BAC transgenic mouse line: A tool for highly efficient gene deletion in retinal progenitor cells. *Genesis* 45:502–507.
34. Inoue T, et al. (2006) Cloning and characterization of mr-s, a novel SAM domain protein, predominantly expressed in retinal photoreceptor cells. *BMC Dev Biol* 6:15.
35. Omori Y, et al. (2011) Analysis of transcriptional regulatory pathways of photoreceptor genes by expression profiling of the Otx2-deficient retina. *PLoS One* 6:e19685.
36. Blackshaw S, et al. (2004) Genomic analysis of mouse retinal development. *PLoS Biol* 2:E247.
37. Hlawatsch J, et al. (2013) Sterile alpha motif containing 7 (samd7) is a novel crx-regulated transcriptional repressor in the retina. *PLoS One* 8:e60633.
38. Jeon CJ, Strettoi E, Masland RH (1998) The major cell populations of the mouse retina. *J Neurosci* 18:8936–8946.
39. Applebury ML, et al. (2000) The murine cone photoreceptor: A single cone type expresses both S and M opsins with retinal spatial patterning. *Neuron* 27:513–523.
40. Akhmedov NB, et al. (2000) A deletion in a photoreceptor-specific nuclear receptor mRNA causes retinal degeneration in the rd7 mouse. *Proc Natl Acad Sci USA* 97:5551–5556.
41. Kim CA, Gingery M, Pilpa RM, Bowie JU (2002) The SAM domain of polyhomeotic forms a helical polymer. *Nat Struct Biol* 9:453–457.
42. Isono K, et al. (2013) SAM domain polymerization links subnuclear clustering of PRC1 to gene silencing. *Dev Cell* 26:565–577.
43. Kawate T, Gouaux E (2006) Fluorescence-detection size-exclusion chromatography for precrystallization screening of integral membrane proteins. *Structure* 14:673–681.
44. Peterson AJ, et al. (1997) A domain shared by the Polycomb group proteins Scm and ph mediates heterotypic and homotypic interactions. *Mol Cell Biol* 17:6683–6692.
45. Kim CA, Sawaya MR, Cascio D, Kim W, Bowie JU (2005) Structural organization of a sex-comb-on-midleg/polyhomeotic copolymer. *J Biol Chem* 280:27769–27775.
46. Baker KD, Beckstead RB, Mangelsdorf DJ, Thummel CS (2007) Functional interactions between the Moses corepressor and DHR78 nuclear receptor regulate growth in Drosophila. *Genes Dev* 21:450–464.
47. Schneiderman JI, Goldstein S, Ahmad K (2010) Perturbation analysis of heterochromatin-mediated gene silencing and somatic inheritance. *PLoS Genet* 6:e1001095.
48. Pirrotta V, Li HB (2012) A view of nuclear Polycomb bodies. *Curr Opin Genet Dev* 22:101–109.
49. Gao Z, et al. (2012) PCGF homologs, CBX proteins, and RYBP define functionally distinct PRC1 family complexes. *Mol Cell* 45:344–356.
50. Blackledge NP, et al. (2014) Variant PRC1 complex-dependent H2A ubiquitylation drives PRC2 recruitment and Polycomb domain formation. *Cell* 157:1445–1459.
51. Eskeland R, et al. (2010) Ring1B compacts chromatin structure and represses gene expression independent of histone ubiquitination. *Mol Cell* 38:452–464.
52. Peterson AJ, et al. (2004) Requirement for sex comb on midleg protein interactions in Drosophila Polycomb group repression. *Genetics* 167:1225–1239.
53. Roseman RR, et al. (2001) Long-range repression by multiple Polycomb group (PcG) proteins targeted by fusion to a defined DNA-binding domain in Drosophila. *Genetics* 158:291–307.
54. Irie S, et al. (2015) Rax homeoprotein regulates photoreceptor cell maturation and survival in association with Crx in the postnatal mouse retina. *Mol Cell Biol* 35:2583–2596.
55. Müller J, Kassis JA (2006) Polycomb response elements and targeting of Polycomb group proteins in Drosophila. *Curr Opin Genet Dev* 16:476–484.
56. Frey F, et al. (2016) Molecular basis of PRC1 targeting to Polycomb response elements by PhoRC. *Genes Dev* 30:1116–1127.
57. Ren X, Kerppola TK (2011) REST interacts with Cbx proteins and regulates Polycomb repressive complex 1 occupancy at RE1 elements. *Mol Cell Biol* 31:2100–2110.
58. Yu M, et al. (2012) Direct recruitment of Polycomb repressive complex 1 to chromatin by core binding transcription factors. *Mol Cell* 45:330–343.
59. Trimarchi JM, Fairchild B, Wen J, Lees JA (2001) The E2F6 transcription factor is a component of the mammalian Bmi1-containing Polycomb complex. *Proc Natl Acad Sci USA* 98:1519–1524.
60. Simon JA, Kingston RE (2013) Occupying chromatin: Polycomb mechanisms for getting to genomic targets, stopping transcriptional traffic, and staying put. *Mol Cell* 49:808–824.
61. Lem J, et al. (1999) Morphological, physiological, and biochemical changes in rhodopsin knockout mice. *Proc Natl Acad Sci USA* 96:736–741.
62. Chakraborty D, Conley SM, Naash MI (2013) Overexpression of retinal degeneration slow (RDS) protein adversely affects rods in the rd7 model of enhanced S-cone syndrome. *PLoS One* 8:e63321.
63. Bernal S, et al. (2008) Analysis of the involvement of the NR2E3 gene in autosomal recessive retinal dystrophies. *Clin Genet* 73:360–366.
64. Van Schil K, et al. (2016) Autosomal recessive retinitis pigmentosa with homozygous rhodopsin mutation E150K and non-coding cis-regulatory variants in CRX-binding regions of SAMD7. *Sci Rep* 6:21307.
65. Muranishi Y, et al. (2011) An essential role for RAX homeoprotein and NOTCH-HES signaling in Otx2 expression in embryonic retinal photoreceptor cell fate determination. *J Neurosci* 31:16792–16807.
66. Haider NB, et al. (2006) The transcription factor Nr2e3 functions in retinal progenitors to suppress cone cell generation. *Vis Neurosci* 23:917–929.
67. Hasegawa K, et al. (2015) SCML2 establishes the male germline epigenome through regulation of histone H2A ubiquitination. *Dev Cell* 32:574–588.
68. Bonasio R, et al. (2014) Interactions with RNA direct the Polycomb group protein SCML2 to chromatin where it represses target genes. *eLife* 3:e02637.
69. Ueno S, et al. (2005) Physiological function of S-cone system is not enhanced in rd7 mice. *Exp Eye Res* 81:751–758.
70. Sanuki R, Omori Y, Koike C, Sato S, Furukawa T (2010) Panky, a novel photoreceptor-specific ankyrin repeat protein, is a transcriptional cofactor that suppresses CRX-regulated photoreceptor genes. *FEBS Lett* 584:753–758.
71. Sato S, et al. (2008) Pikachurin, a dystroglycan ligand, is essential for photoreceptor ribbon synapse formation. *Nat Neurosci* 11:923–931.
72. Sanuki R, et al. (2011) miR-124a is required for hippocampal axogenesis and retinal cone survival through Lhx2 suppression. *Nat Neurosci* 14:1125–1134.
73. Koike C, et al. (2007) Functional roles of Otx2 transcription factor in postnatal mouse retinal development. *Mol Cell Biol* 27:8318–8329.
74. Isono K, et al. (2005) Mammalian polyhomeotic homologues Phc2 and Phc1 act in synergy to mediate Polycomb repression of Hox genes. *Mol Cell Biol* 25:6694–6706.
75. Lee TI, Johnstone SE, Young RA (2006) Chromatin immunoprecipitation and microarray-based analysis of protein location. *Nat Protoc* 1:729–748.
76. Katoh K, et al. (2010) Blimp1 suppresses Chx10 expression in differentiating retinal photoreceptor precursors to ensure proper photoreceptor development. *J Neurosci* 30:6515–6526.